Diffuse cliques maintain biodiversity in species-rich ecological communities

Matthieu Barbier[1,3*], Claire de Mazancourt[1], Michel Loreau[1] and Guy Bunin[2]

May 28, 2019

High-dimensional phenomena, which often defy low-dimensional intuitions[1;2], are an essential and yet seldom explored frontier in our understanding of ecological communities[3]. Ecologists have long speculated about how large numbers of species manage to coexist in rich assemblages. Most answers to date have focused on identifying particular dimensions along which species may organize to persist together[4]. Here we instead ask: what is the characteristic structure of a community where coexistence arises from a large number of concurrent factors? In such communities, individual species might not follow any evident pattern in their interactions, yet the group as a whole exhibits a statistical structure that we call "diffuse clique". We find remarkable quantitative evidence for this pattern across a range of plant biodiversity experiments. Our approach exploits the emergent simplicity of high-dimensional systems[5;6], a powerful idea originating in physics that has, so far, rarely been demonstrated unequivocally in ecological data. We conclude that a subtle form of collective order may underlie complex networks of species interactions. This diffuse order offers a new grasp on how ecological communities maintain their fascinating diversity.

The coexistence of many species with similar attributes is a long-standing puzzle: simple theories and experiments support the principle of competitive exclusion, whereby the best competitor should displace all others[7;8]. Yet, strict dominance by one species appears, at most spatial and temporal scales, to be the exception rather than the rule in the natural world. Over decades of ecological research, many partial solutions to this puzzle have been proposed, and integrated into the overarching framework of niche theory[9]. This framework suggests that we should identify particular trade-offs between abilities such as resource exploitation[10], defense against predators[11] and tolerance of temporal fluctuations[12;13]. Through these trade-offs, strict bounds are imposed upon how species grow and interact, preventing any species from overwhelming its competitors.

We propose to start from a different perspective. Coexistence in highly diverse communities likely involves a large number of niches and trade-offs, some known and many unknown *a priori*[14]. Each cross-species interaction may be determined by a unique combination of factors, precluding any simple and conspicuous (low-dimensional) order in the community[3]. Some ecological theories therefore make the assumption that interactions are essentially random[5] – a bold move, yet one that parallels major successes in physics[15;16]. Fully random interactions, however, do not allow many species to coexist[17]. The high biodiversity observed in many natural communities therefore implies some form of latent structure.

We first derive a theoretical prediction, the most parsimonious way to constrain species interactions in order to achieve coexistence. We uncover it by asking: if one samples many different interaction networks, and retains only those where all species survive, what do the remaining networks have in common? Some may appear very structured, others almost random. Yet, we find in Fig. 1 that *most* of these networks exhibit the same statistical pattern. This pattern, expressed in equations below, is a weak but crucial bias in how the most successful competitors interact with others[20]. We now derive this pattern from a simpler probabilistic argument, and explain in intuitive terms how it allows coexistence.

Measuring species interactions is often difficult and prone to high uncertainty[21–23], and most empirical settings only give us access to aggregated statistics. The total effect of interactions on one species i can be inferred from its *relative yield*

$$\eta_i = B_i/K_i \tag{1}$$

the ratio of its abundance B_i in a community to its abun-

* Corresponding author: contact@mrcbarbier.org.
[1] Centre for Biodiversity Theory and Modelling, Theoretical and Experimental Ecology Station, UMR 5321, CNRS and Paul Sabatier University, 09200 Moulis, France. [2] Department of Physics, Technion-Israel Institute of Technology, Haifa, 3200003 Israel. [3] Institut Natura e Teoria Pirenèus, 75015 Paris, France.

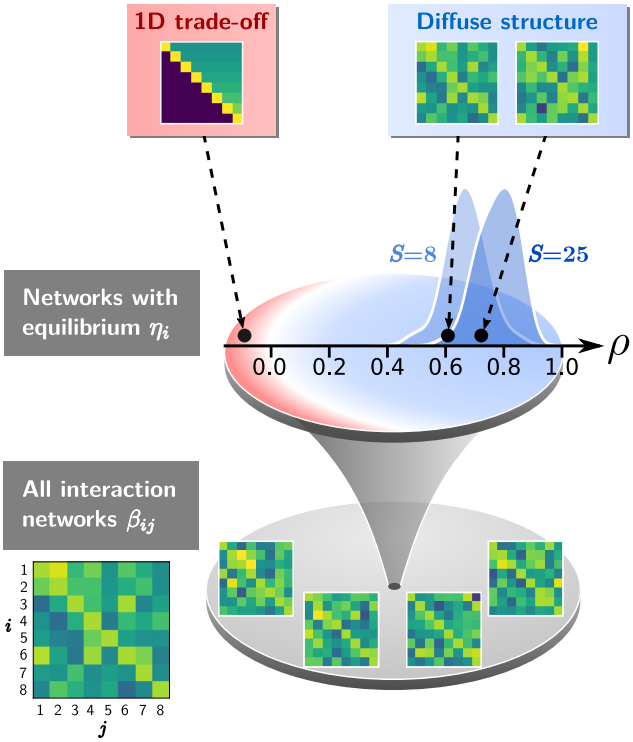

Figure 1: **Finding a general pattern of coexistence in species-rich interaction networks.** Interaction networks of S species are represented by $S \times S$ matrices (square boxes) where each element β_{ij} denotes the effect of species j on species i. Of all possible species interaction networks (bottom disk), only an infinitesimal fraction (shaded area) allows S species to coexist at some equilibrium η_i. Zooming into this area of coexistence (upper disk), we find that most such networks appear almost random, yet they tend to follow a common trend which we call a "diffuse clique structure": an underlying pattern of biases (4) and correlations (6) hidden in the large spread of coefficients β_{ij}. We define a metric ρ to quantify how well our predicted pattern is observed in a given interaction network. We find in simulations that this metric ρ gets closer to 1 as biodiversity increases (histograms show the distribution of ρ for 200 networks with $S = 8$ and 25 species). By contrast, some coexistence mechanisms, such as the one-dimensional competition-colonization tradeoff [18;19], can give rise to highly atypical networks, showing unrelated or even opposite patterns.

dance without competitors K_i (known as carrying capacity) in the same environment [9]. We interpret species with higher η as *successful* competitors, as they benefit more (or suffer less) in total from their interactions with others. The simplest way to model these interactions is by assuming a linear dependence between species

$$\eta_i = 1 - \sum_{j \neq i} \beta_{ij} \eta_j \qquad \text{for all } i. \tag{2}$$

where β_{ij} is the competitive effect of species j on species i. This relationship, which can be tested empirically [24;25], holds between coexisting species at equilibrium in the classic Lotka-Volterra model.

Many different interaction networks can generate the same equilibrium community. Observing the coexistence of S species with relative yields η_i conveys some information about their interactions, but not enough to fully determine them: the equations (2) impose S constraints, while there are $S(S-1)$ unknown interaction coefficients β_{ij}. On the other hand, community-wide statistics, such as the mean strength of competition $\bar{\beta}$, can be reliably deduced from that information [26] (Appendix E).

We therefore adopt a probabilistic approach, and ask what is the *most likely* community structure, i.e. the set of features most widely shared among the many possible solutions. We first define a prior distribution $P(\beta_{ij})$ that can be adapted to our biological knowledge of the community. For all experiments below, we simply assume that each coefficient β_{ij} is drawn independently from a normal distribution with mean $\bar{\beta}$. We then compute how this prior is modified once restricted to networks that admit the equilibrium η_i (Appendix B). Computing a posterior distribution given a prior and linear constraints (2) is a well-established problem in probability theory [27;28].

We find that interactions β_{ij} should follow two statistical patterns that both admit intuitive interpretations (Fig. 2). First, competition must be biased to explain which species are successful or not. If all interaction strengths were equal to the prior mean, $\beta_{ij} = \bar{\beta}$, we would expect any species to achieve the same relative yield,

$$\eta^* = \frac{1 - \bar{\beta} \sum_i \eta_i}{1 - \bar{\beta}}. \tag{3}$$

When $\eta_i > \eta^*$, we therefore expect that species i suffers less competition than $\bar{\beta}$, and conversely if $\eta_i < \eta^*$. In our calculation, this appears in the conditional expectation of the competitive effect of j on i,

$$\mathrm{E}[\beta_{ij} | \eta_i, \eta_j] = \bar{\beta} + (1 - \bar{\beta}) \Delta(\eta_i, \eta_j) \tag{4}$$

which deviates from the prior mean $\bar{\beta}$ by a bias

$$\Delta(\eta_i, \eta_j) = -\frac{(\eta_i - \eta^*)\eta_j}{\sum_{m \neq i} \eta_m^2}. \tag{5}$$

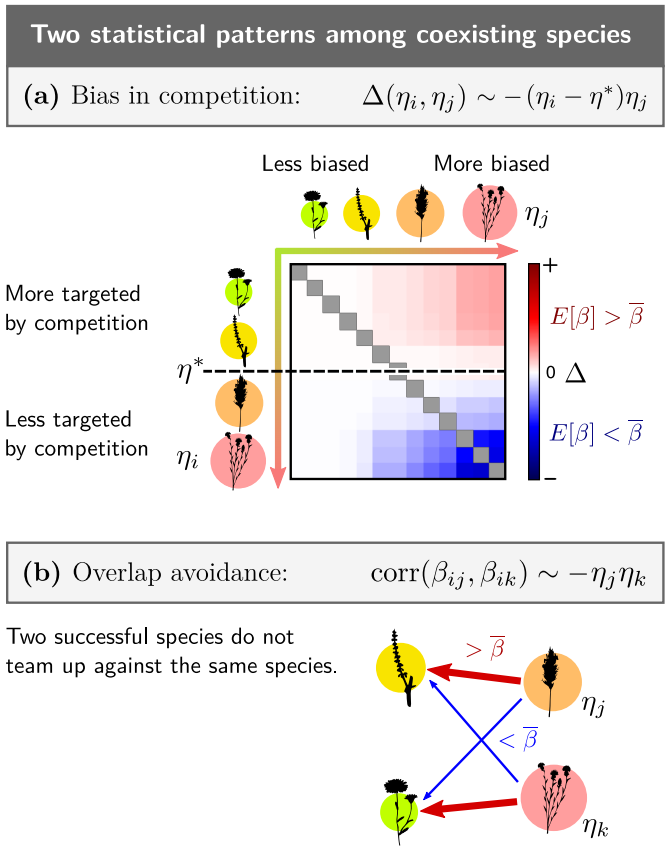

Figure 2: **The diffuse clique structure is characterized by two statistical patterns in the competition of successful species. (a)** Bias in competitive effects (4). If all species competed with equal strength $\bar{\beta}$, we would expect any given species i to achieve the relative yield $\eta_i = \eta^*$ (3). When η_i differs from this baseline, we can infer how interactions most likely deviate from $\bar{\beta}$. We show this deviation $\Delta(\eta_i, \eta_j)$ for simulated data, in the form of a matrix which we now describe. **Left to right:** a species with low η_j competes indiscriminately against others (white, $\Delta = 0$), whereas a species with high η_j is a biased competitor. **Top to bottom:** species with $\eta_i < \eta^*$ experience stronger competition on average (red, $\Delta > 0$) whereas species with $\eta_i > \eta^*$ experience weaker competition (blue, $\Delta < 0$). Together, these biases indicate the existence of a "clique" of species that compete less against each other, and more against all others, thus achieving higher relative yield than the baseline η^*. **(b)** Correlation structure between columns of the interaction matrix: the competitive effects of two successful species are anti-correlated, avoiding overlap in which species they affect, whereas competition from unsuccessful species is again indiscriminate.

We see that this bias is not evenly distributed. Competition coming from unsuccessful species (low η_j) can be random without compromising the equilibrium. On the other hand, a species that is successful (achieving high η_j) is likely to have biased interactions, competing less on average against other successful species, and experiencing weaker competition from them (Fig. 2a).

The second pattern imposes that successful species j and k avoid competing against the same target i (Fig. 2b)

$$\mathrm{corr}(\beta_{ij}, \beta_{ik} | \eta_i, \eta_j, \eta_k) = -\frac{\eta_j \eta_k}{\sum_{m \neq i} \eta_m^2}. \tag{6}$$

While the first pattern (4) determines the *expected* success of each species, the second pattern guarantees that each relative yield is *exactly* set to η_i. We show in Appendix B that this correlation pattern prevents η_i from deviating from its expectation, which would likely drive some low-η species to extinction in a fully random community.

Taken together, these two patterns suggest that we will generally observe a fuzzy "clique" of competitors that are both biased and successful, surrounded by unsuccessful species with arbitrary interactions. This picture differs in multiple respects from classic explanations of coexistence. It does not suppose a measurable segregation of species into distinct niches. By imposing only the weakest possible constraints upon the many degrees of freedom in β_{ij}, it allows interactions to take almost arbitrary values. It also represents a form of collective organization, where coexistence arises, not from particular species traits, but from statistical biases distributed over all interactions. Accordingly, Fig. 1 shows that this structure becomes increasingly prevalent (although more diffuse) in highly diverse communities.

We now present an empirical validation of these patterns on experimental data in Fig. 3 and Fig. 4. Grassland biodiversity experiments[29–31] provide an ideal testbed for inferring species interactions and mechanisms of coexistence. Each experiment contains a large number of plots in which plant species are assembled in varying numbers and combinations, out of a pool of $S = 8$ to 60 species depending on the experiment. Biomass in monoculture (single-species plots) provides an estimate of the species' carrying capacities.

To test our predictions, we split these data in two sets. Relative yields η_i in the full-diversity plots are used to compute the theoretical expectations (4) and correlations (6) of interactions. All other plots, comprising different subsets of the species pool, are used to fit individual interaction coefficients β_{ij} by a multilinear regression of equation (2). From these fitted coefficients, we construct empirical estimates of the theoretical statistics.

We show in Fig. 3 the interaction matrix computed in the Wageningen grassland experiment. While lacking ap-

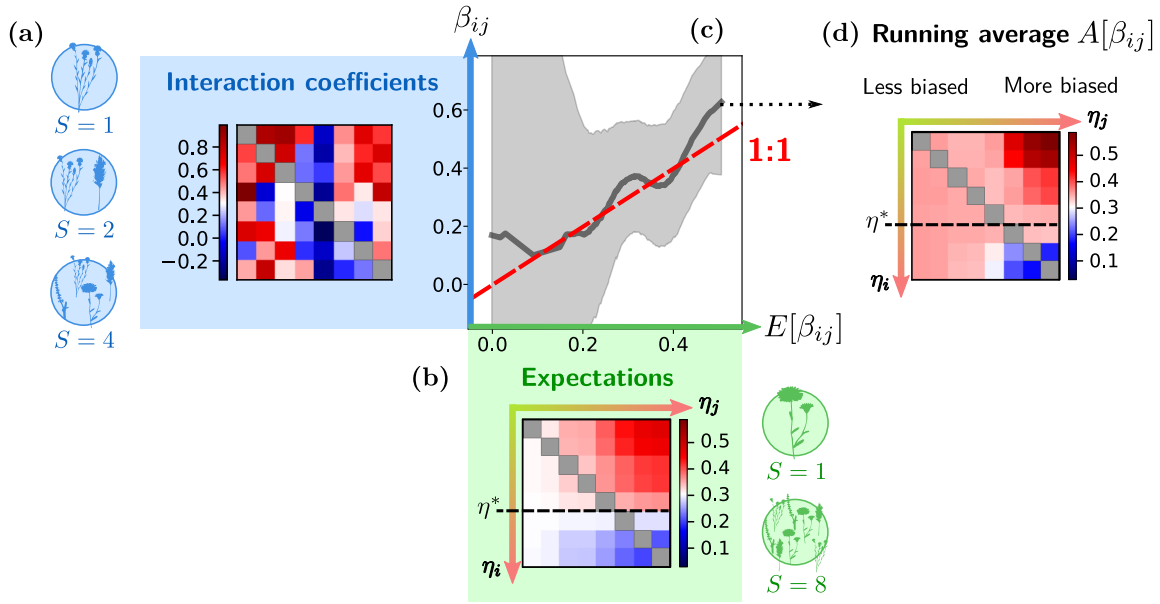

Figure 3: **Diffuse clique in the Wageningen grassland experiment.** **(a)** Using many species combinations (56 sets of $S < 8$ species), we can fit interaction coefficients β_{ij} by multilinear regression[23]. **(b)** Knowing only the relative yields η_i in the full community (all $S = 8$ species), our method (4) suggests a theoretical expectation for each interaction, $E[\beta_{ij}|\eta_i, \eta_j]$. **(c)** Comparison between fitted coefficients and expectations. In our diffuse pattern, individual coefficients are expected to exhibit a large spread around their expectation $E[\beta_{ij}]$. But we can construct an empirical estimate of the mean, the running average $A[\beta_{ij}]$ (grey curve, 90% CI in shaded area). It is in good agreement with the theoretical mean, as shown by proximity to the red 1:1 line. **(d)** We show this empirical average $A[\beta_{ij}]$ in matrix form (median value for each species pair i, j), to compare with the predicted matrix $E[\beta_{ij}]$ in (b).

parent structure, it conforms to the statistical patterns predicted by our theory. Individual coefficients β_{ij} show a wide dispersion (Fig. 3), which may be widened by inference errors[23]. Despite this large spread, when we group interactions involving species with similar relative yields, their average $A[\beta_{ij}|\eta_i, \eta_j]$ lays close to a one-to-one relationship with the theoretical expectation $E[\beta_{ij}|\eta_i, \eta_j]$. The reconstructed statistical pattern in Fig. 3 agrees both qualitatively and quantitatively with the predictions.

This striking agreement between theory and data is quantified for multiple experiments in Fig. 4. We stress that this is a strong test. All results are fully determined by measured abundances, without any adjustable parameter. Furthermore, none of the data used to parameterize theoretical formulas is involved in fitting the empirical interaction coefficients. Finally, we rule out these relationships being artefacts of our method, as they vanish for very sparse or noisy data, and can be violated in simulated ecosystems with a low-dimensional structure, as seen in Fig. 1 and 4.

The approach developed here provides a test of how *typical* an empirical or theoretical interaction network is, given the observed abundances of its species: how similar it is to the majority of possible networks admitting the same equilibrium η_i (Fig. 1). We also detail in Appendix B an algorithm for generating such typical networks. A deviation from typicality may hint at low dimensional mechanisms, such as particular trade-offs[4].

We have introduced a novel methodology for thinking about the collective organization of coexistence in ecological communities. This approach goes beyond the particular theoretical predictions (4) and (6), which are simplified results tied to our choice of unstructured prior distribution and linear interactions. When there is a positive but nonlinear relationship between data and predictions, our approach could be improved with more accurate inference and more realistic models, but it already captures an important qualitative feature of community organization. The same methods could be expanded by adding structure to the prior and nonlinearity to the dynamics. This will allow extensions to more complex communities, such as food webs, or networks that have been structured by other ecological and evolutionary processes[32]. Future work should explore how this approach, based on ideas from statistical physics and generic properties of high-dimensional systems, can be generalized to other biological systems.

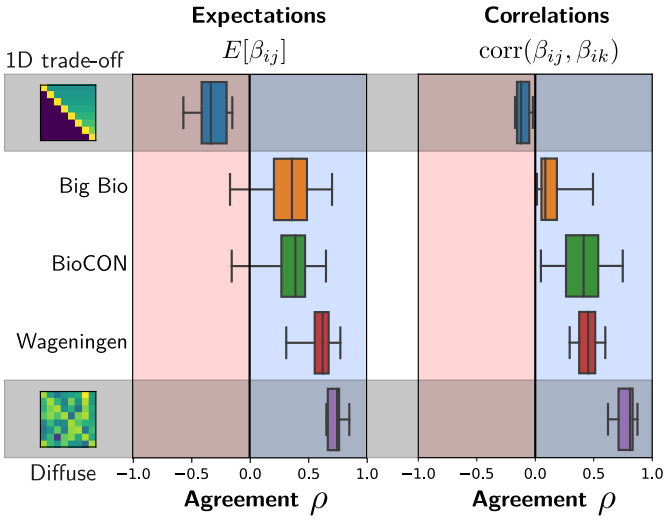

Figure 4: **Cross-experiment validation of the two components of the diffuse clique structure.** We compute the agreement between the measured and predicted values for: conditional expectations $E[\beta_{ij}|\eta_i, \eta_j]$ (left) and correlations $\mathrm{corr}(\beta_{ij}, \beta_{ik}|\eta_i, \eta_j, \eta_k)$ (right), using the predictions in Fig. 2. We show the agreement metric ρ (see SI Appendix E), comprised between -1 and 1. Boxes and whiskers represent the 50% and 95% CI of bootstrapped values, with the median shown as the center line. The shaded rows show results for two coexistence mechanisms as in Fig. 1: a one-dimensional trade-off with $\rho < 0$ (top row) and our high-dimensional diffuse clique structure with $\rho > 0$ (bottom row), both aggregated over 5 simulated communities with $S = 25$ species. In the Wageningen experiment, ρ is significantly larger than zero for both means and correlations. The Big Bio and BioCON experiments comprise multiple treatments (see SI Appendix E), over which we aggregate to find that zero always lies below the 10th percentile of ρ.

Methods

Experimental data

We employ data from 3 grassland biodiversity experiments in Wageningen, Netherlands[29] and Cedar Creek, MN, USA (the Big Biodiversity[31] and BioCON[30] experiments). Each experiment uses a pool of species seeded or planted in various combinations, including some or all possible monocultures ($S = 1$ species), some partial compositions, and all species planted together. We removed the first two year for all experiments as they showed clear evidence of transient dynamics (Appendix C).

Interactions measured in the Wageningen experiment showed much lower inference error than in other experiments. Therefore, we used this experiment to assess our hypothesis that observed abundances are primarily determined by fixed inter-species interactions (Appendix D). The consistency of the equilibrium Lotka-Volterra description (2) was shown through a series of tests: we employed multiple inference procedures for the matrix β_{ij} and carrying capacities K_i, using different subsets of the data for prediction and validation, and found them all statistically significant and in agreement within empirical uncertainty. In particular, carrying capacities K_i inferred from all multispecies plots ($S > 1$) agreed with measurements in monocultures ($S = 1$). Likewise, interactions β_{ij} inferred from all plots with $S < 8$ were consistent with the equilibrium values of $\eta_i = B_i/K_i$ in octoculture ($S = 8$). This strongly supports the simple linear model (2). Interaction estimates from other experiments were less robust and might be affected by nonlinearity, transient dynamics, stochasticity and errors.

Validation of theoretical predictions

For each experiment, we first split monoculture ($S = 1$) replicates in two sets, and compute the species' carrying capacities K_i for each set, to be used separately. For a maximal plot biodiversity $S_{\max}$, all plots with $1 < S < S_{\max}$ and the first set of monocultures were used to infer the interaction matrix β_{ij} using the hyperplane (multilinear) least-squares fit proposed by Xiao et al[23] (see Appendix D). The second set of monocultures and the species abundance B_i in plots with $S = S_{\max}$ were then used compute the relative yields $\eta_i = B_i/K_i$ in the full community. All calculations were performed 250 times, using different bootstrapped sample means as values for K_i and B_i. Each calculation led to a different set of η_i, β_{ij} and $\overline{\beta}$ (see Appendix A for calculation details).

We tested the two components of the diffuse clique pattern, starting with the pattern of means (4). We plotted the measured values of β_{ij} (hereafter y) against their the-

oretical expectation $E[\beta_{ij}|\eta_i, \eta_j]$ (hereafter x). To obtain an empirical estimate of the expectation for a single interaction coefficient, we performed a running average: for each point (x, y), we replaced its y coordinate by the average $\overline{y}$ within a window centered on x and spanning 10% of the x-axis; we also measure the 90% CI over bootstrapped values (Fig. 3c). We then grouped all values $\overline{y}$ associated with the same species pair (i, j), took their median, and reconstructed an empirical matrix of expectations B_{ij} (shown in Fig. 3d).

To construct a stringent test (see SI Appendix E), the metric of agreement ρ used in Fig. 1 and 4 is defined as the minimum of three correlation scores: ρ_0 testing the overall relationship between x and $\overline{y}$, ρ_{row} testing the agreement of row-wise trends (within bins of η_i) and ρ_{col} for column-wise trends (within bins of η_j). This ensures that all the qualitative features described in Fig. 2 are present, and reduces the risk of spurious agreement scores.

We proceeded similarly to test the pattern of correlations (6). Defining $d_{ij} = \beta_{ij} - E[\beta_{ij}|\eta_i, \eta_j]$, we compute $y = \delta_{jk} - d_{ij}d_{ik}/\text{mean}\left(d_{mn}^2\right)$, where $\delta_{jk} = 1$ if $j = k$ and 0 otherwise, and the denominator is the sample mean. We then plotted y against the prediction $x = -\eta_j\eta_k/\sum_{l\neq i}\eta_l^2$, performed a running average to get $\overline{y}$, and constructed an empirical tensor of correlations C_{ijk} from the median of all values associated with each species triplet (i, j, k).

Data availability

This study brought together existing data that was obtained upon request (Wageningen biodiversity experiment data from J. van Ruijven[29]) and data that is publicly available (Big Bio `http://www.cedarcreek.umn.edu/research/data` and BioCON `http://www.biocon.umn.edu/`). Data represented in Fig. 3 and 4 is available at `https://github.com/mrcbarbier/diffuseclique`.

Code availability

Computer code developed for this study is available at `https://github.com/mrcbarbier/diffuseclique`.

Acknowledgments

We thank J.-F. Arnoldi, Y. Zelnik and F. Isbell for comments. Our gratitude goes to J. van Ruijven for sharing data from the Wageningen experiment. Experimental work at Cedar Creek was supported by grants from the US National Science Foundation Long-Term Ecological Research Program (LTER) including DEB-0620652 and DEB-1234162, and further support was provided by the Cedar Creek Ecosystem Science Reserve and the University of Minnesota. M.B., C.d.M. and M.L. were supported by the TULIP Laboratory of Excellence (ANR-10-LABX-41) and by the BIOSTASES Advanced Grant, funded by the European Research Council under the European Union's Horizon 2020 research and innovation programme (666971). G.B. was supported by the Israel Science Foundation (ISF) Grant no. 773/18.

Author contributions

G.B. developed the theoretical approach. M.B., G.B. and C.d.M. analyzed the data. M.B. wrote the first draft. All authors contributed substantially to study design and manuscript revisions.

References

[1] Jorge Kurchan and Laurent Laloux. Phase space geometry and slow dynamics. *Journal of Physics A: Mathematical and General*, 29(9):1929, 1996.

[2] Mikhail Tikhonov and Remi Monasson. Innovation rather than improvement: a solvable high-dimensional model highlights the limitations of scalar fitness. *Journal of Statistical Physics*, pages 1–31, 2018.

[3] James S Clark, Mike Dietze, Sukhendu Chakraborty, Pankaj K Agarwal, Ines Ibanez, Shannon LaDeau, and Mike Wolosin. Resolving the biodiversity paradox. *Ecology Letters*, 10(8):647–659, 2007.

[4] Adam Thomas Clark, Clarence Lehman, and David Tilman. Identifying mechanisms that structure ecological communities by snapping model parameters to empirically observed tradeoffs. *Ecology letters*, 21(4):494–505, 2018.

[5] Robert M May. Will a large complex system be stable? *Nature*, 238:413–414, 1972.

[6] Matthieu Barbier, Jean-François Arnoldi, Guy Bunin, and Michel Loreau. Generic assembly patterns in complex ecological communities. *Proceedings of the National Academy of Sciences*, 115(9):2156–2161, 2018.

[7] GF Gause. The struggle for existence. *Williams and Wilkins, Baltimore*, 1934.

[8] David Tilman. *Resource competition and community structure*. Princeton University Press, 1982.

[9] Michel Loreau. *From populations to ecosystems: Theoretical foundations for a new ecological synthesis (MPB-46)*. Princeton University Press, 2010.

[10] Robert MacArthur. Species packing, and what competition minimizes. *Proceedings of the National Academy of Sciences*, 64(4):1369–1371, 1969.

[11] Simon A Levin. Community equilibria and stability, and an extension of the competitive exclusion principle. *The American Naturalist*, 104(939):413–423, 1970.

[12] Peter Chesson. Quantifying and testing coexistence mechanisms arising from recruitment fluctuations. *Theoretical population biology*, 64(3):345–357, 2003.

[13] György Barabás, Rafael D'Andrea, and Simon Maccracken Stump. Chesson's coexistence theory. *Ecological Monographs*, 2018.

[14] Benoît Jaillard, Camille Richon, Philippe Deleporte, Michel Loreau, and Cyrille Violle. An a posteriori species clustering for quantifying the effects of species interactions on ecosystem functioning. *Methods in Ecology and Evolution*, 9(3):704–715, 2018.

[15] Eugene P Wigner. On the distribution of the roots of certain symmetric matrices. *Annals of Mathematics*, pages 325–327, 1958.

[16] Philip W Anderson. Absence of diffusion in certain random lattices. *Physical review*, 109(5):1492, 1958.

[17] Serguei Saavedra, Rudolf P Rohr, Jordi Bascompte, Oscar Godoy, Nathan JB Kraft, and Jonathan M Levine. A structural approach for understanding multispecies coexistence. *Ecological Monographs*, 87(3):470–486, 2017.

[18] Richard Levins and David Culver. Regional coexistence of species and competition between rare species. *Proceedings of the National Academy of Sciences*, 68(6):1246–1248, 1971.

[19] David Tilman. Competition and biodiversity in spatially structured habitats. *Ecology*, 75(1):2–16, 1994.

[20] Guy Bunin. Interaction patterns and diversity in assembled ecological communities. *arXiv preprint arXiv:1607.04734*, 2016.

[21] Claire Mazancourt, Forest Isbell, Allen Larocque, Frank Berendse, Enrica Luca, James B Grace, Bart Haegeman, H Wayne Polley, Christiane Roscher, Bernhard Schmid, et al. Predicting ecosystem stability from community composition and biodiversity. *Ecology letters*, 16(5):617–625, 2013.

[22] Charles K Fisher and Pankaj Mehta. Identifying keystone species in the human gut microbiome from metagenomic timeseries using sparse linear regression. *PloS one*, 9(7):e102451, 2014.

[23] Yandong Xiao, Marco Tulio Angulo, Jonathan Friedman, Matthew K Waldor, Scott T Weiss, and Yang-Yu Liu. Mapping the ecological networks of microbial communities. *Nature communications*, 8(1):2042, 2017.

[24] Daniel S Maynard, J Timothy Wootton, Carlos A Serván, and Stefano Allesina. Reconciling empirical interactions and species coexistence. *Ecology letters*, 2019.

[25] Daniel S Maynard, Zachary R Miller, and Stefano Allesina. Predicting coexistence in experimental ecological communities. *bioRxiv*, page 598326, 2019.

[26] Hugo Fort. Quantitative predictions from competition theory with an incomplete knowledge of model parameters tested against experiments across diverse taxa. *Ecological Modelling*, 368:104–110, 2018.

[27] Edwin T Jaynes. On the rationale of maximum-entropy methods. *Proceedings of the IEEE*, 70(9):939–952, 1982.

[28] Frédéric Vrins. Sampling the multivariate standard normal distribution under a weighted sum constraint. *Risks*, 6(3):64, 2018.

[29] Jasper Van Ruijven and Frank Berendse. Long-term persistence of a positive plant diversity–productivity relationship in the absence of legumes. *Oikos*, 118(1):101–106, 2009.

[30] Peter B Reich, David Tilman, Shahid Naeem, David S Ellsworth, Johannes Knops, Joseph Craine, David Wedin, and Jared Trost. Species and functional group diversity independently influence biomass accumulation and its response to CO2 and N. *Proceedings of the National Academy of Sciences*, 101(27):10101–10106, 2004.

[31] David Tilman, Peter B Reich, and Johannes MH Knops. Biodiversity and ecosystem stability in a decade-long grassland experiment. *Nature*, 441(7093):629, 2006.

[32] Sergi Valverde, Jordi Piñero, Bernat Corominas-Murtra, Jose Montoya, Lucas Joppa, and Ricard Solé. The architecture of mutualistic networks as an evolutionary spandrel. *Nature ecology & evolution*, 2(1):94, 2018.